Bibliographical reference

Higher Order Finite and Infinite Acoustical Elements Based on Ultraspherical Polynomials, J. Biermann and O. Von Estorff, Acta Acustica **vol. 99** (Number 5), 2013, pp. 759-769

DOI

https://doi.org/10.3813/AAA.918654

ACTA ACUSTICA UNITED WITH ACUSTICA
Vol. 99 (2013) 759–769

DOI 10.3813/AAA.918654

Higher Order Finite and Infinite Acoustical Elements Based on Ultraspherical Polynomials

J. Biermann[1)], O. von Estorff[2)]

[1)] BMW AG, Acoustics, Mechatronic Systems, 80788 Munich, Germany, jan.biermann@bmw.de

[2)] Institute of Modelling and Computation, Hamburg University of Technology, Denickestraße 17, 21073 Hamburg, Germany. estorff@tuhh.de

Summary

This paper deals with the simulation of interior as well as exterior acoustical phenomena in the mid to high frequency range using the finite/infinite element method. In terms of controlling the pollution effect it is relied on the *p*-FEM concept. Due to this modeling approach the resulting parameterized linear system of equation is sparse, complex valued, indefinite, and unsymmetrical. This usually renders challenging when Krylov subspace based iterative solvers are used for the solution step. That is why the focus of this paper is to change the basis of the polynomial finite element aproximation space in order to obtain a favourable spectrum of the system matrix at higher wave numbers and in turn to improve the rate of convergence. As a result a formulations based on ultraspherical polynomials has been developed and numerical test show that this indeed renders faster solver convergence and hence a computationally more efficient simulation.

PACS no. 43.20.El, 43.20.Fn, 43.40.Rj

1. Introduction

The challenge of efficiently obtaining accurate solutions for the Helmholtz equation at elevated frequencies is still unsolved [1]. This is strongly linked to the nature of the indefinite Helmholtz operator, which loses ellipticity with increasing frequency. Hence, it is crucial to sufficiently resolve the wave character of the solution. It is long known that the approximation of the solution with standard finite element methods with low-order piecewise polynomials suffers from the pollution effect [2, 3, 4] which causes spurious dispersion in the computation. Since the dispersion not only affects the accuracy but also the stability [5], it is crucial to control the dispersion error. Theoretically, this could be achieved by classical h-refinement but this approach renders prohibitively expensive[1]. That is why a vast of different methods have been developed in the past years to represent the wave phenomena on a subgrid scale to cope with the dispersion problem more efficiently. All these approaches can be distingushed in different ways. One way is by the type of space used to represend the fine scales, which certainly has a major influence on the accuracy of the discretization. A rather natural and promising way is to incorporate analytical knowledge of the problem into the approximation space, e.g. plane waves in the case of the Helmholtz equation [7, 8, 9]. Not questioning the great potential of this approach, there are still issues if it comes to complex industrial applications and allowing for multiple reflections for example. In that case the direction of wave propagation is not known so it has to be found either iteratively to ensure accuracy [7, 8], or multiple directions have to be allowed in the approximation space like for the GFEM [9, 10]. This not only causes the degrees of freedoms to increase but also leads to the well known conditioning problems of the resulting algrebraic system of equations and hence, shifting the accuracy and stability issue to the solution part of the simulation process. Besides this, integration of complicated trigonometric functions is another burden. The latter one for example is not much of an issue if higher order polynomial spaces are used for the approximation, where accurate integration can be carried out rather efficiently using standard Gauss-quadrature.

Another way of looking at the different methods is how to ensure inter-element continuity. On the one hand bubble functions are used that naturally ensure continuity such as for the Residual Free Bubble approach (RFB) [11], the nearly H^1-optimal Petrov-Galerkin (NOPG) [12] or again the GFEM [9]. On the other hand a discountinous framework can be employed like for the discontinous enrichment method [13, 14, 15, 16] or the ultra weak variational formulation [16, 17, 18].

Finally, the methods can be viewed from the perspective of how the functions for the fine scale approximation are

Received 18 November 2012,
accepted 5 May 2013.

[1] If piecewise linear polynomials are assumed and h is the mesh size, then the necessary condition to ensure the error of the solution at the wave number k being of the same magnitude as the error of best approximation is that k^2h is small [6].Exemplary, if $k^2h < 1$ is claimed, this would imply that the number of degrees of freedom N would be of order $N = O(h^{-3}) = O(k^6)$ [3].

set up. Either they are determined beforehand, like for the classical FEM and for its extension *p*-FEM [19, 20, 21], or the trial/test functions representing the fine scales are determined within a variational multiscale framework [22, 23], i.e. by solving an auxillary variational problem. The RFB and the NOPG fall into the latter category.

All the aforementioned methods aim for an efficient control of the dispersion error by improving the FE-approximation. Undoubtly, in this context all these sophisticated approaches stand out compared to the *p*-FEM concept with locally defined bubbles based on higher order polynomials. But this concept has also proven to give acurate results by reducing the pollution effect [3, 4, 24, 25, 26, 27]. Considering additionall features that are desirable for a certain method, such as simplicity of the concept and its implementation, robustness, and geometric flexibility, it is believed that the *p*-FEM approach is still an appropriate tool and will be used throughout this paper.

The motivation of this work originates from a practical, industrial example, namely the simulation of tire noise [28], which asks for considering the entire simulation process rather than soley focusing on the discretization. That is why the focus of the paper is to rely on the *p*-FEM concept in order to ensure accuracy but to improve the basis of the used piecewise higher order polynomial approximation space in a sense that convergence of Krylov subspace based iterative solvers is enhanced. Certainly, there are various other measures to improve convergence of iterative solvers such as applying sophisticated preconditioning techniques or modifying the solver itself, but these are separate and active fields of research (actually the border between these two mentioned fields is ambiguous) wherefore this issue has been adressed to a separate paper [29]. Furthermore, it is believed that the presented idea is an additional measure to tune the overall performance of the simulation procedure.

The remainder of the paper is organized as follows. In the next section the problem is formally outlined for the sake of completeness and the governing relations are stated. In section 3 the new hierarchical higher order polynomial finite element basis is motivated and presented. Section 4 will demonstrate the effect of the new elements on iterative solvers by using a standard academic example as well as two examples of intustrial size and interest and section 5 willprovide some concluding remarks.

2. Basic formulations

A radiating object B as depicted in Figure 1 is embedded in a bounded acoustic domain Ω with constant fluid properties such as wave speed c and the fluid density ρ. The boundary $\partial\Omega_i$ of Ω is denoted by S and consists of three distinct regions S_D, S_N and S_R, where $S = S_D \cup S_N \cup S_R$ and $S_\mathcal{A} \cap S_\mathcal{B} = \emptyset$ with $\mathcal{A}, \mathcal{B} \in \{D, N, A\}$, $\mathcal{A} \neq \mathcal{B}$ holds.

On S_D, S_N, and S_R Dirichlet, Neumann and Robin boundary conditions are prescribed, respectively. The normal velocity is denoted by v_n and A_n is the normal admittance. The wave number is $k = \omega/c$, where ω represents the angular frequency. The corresponding boundary value problem for the sound pressure p then reads

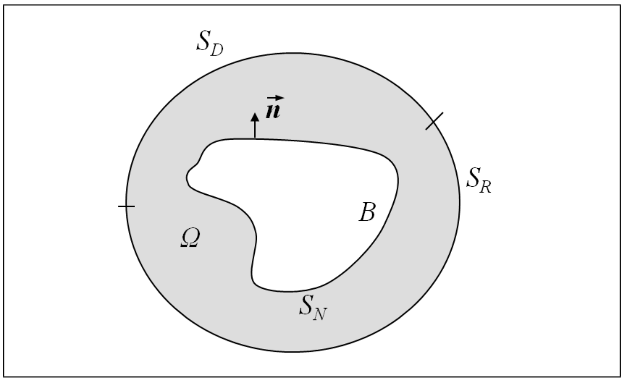

Figure 1. Interior acoustic problem.

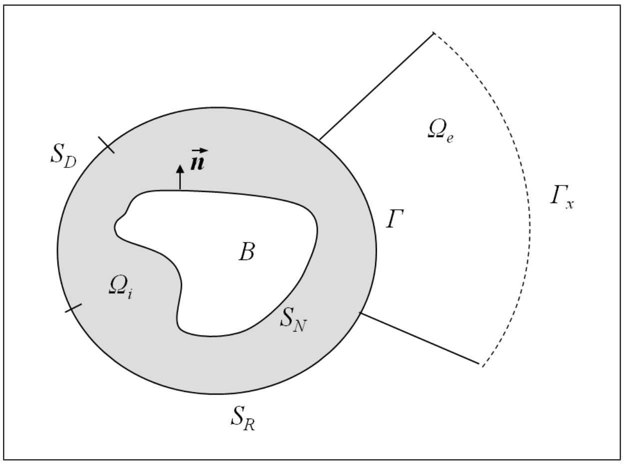

Figure 2. Exterior acoustic problem.

$$\Delta p + k^2 p = 0 \quad \text{in} \quad \Omega \tag{1}$$

$$p = p^o \quad \text{on} \quad S_D \tag{2}$$

$$v_n = v_n^o \quad \text{on} \quad S_N \tag{3}$$

$$\frac{v_n}{p} = A_n \quad \text{on} \quad S_R. \tag{4}$$

If the exterior acoustic case is to be considered (Figure 2), the acoustic domain Ω becomes unbounded and is formally divided into a bounded part Ω_i and a unbounded part Ω_e that share the interface Γ. Γ_x denotes the virtual outer boundary of Ω_e at infinity. Then the set of equations (1) to (4) is to be extended by the Sommerfeld radiation condition

$$\lim_{r\to\infty} r\left(\mathrm{i}kp + \frac{\partial p}{\partial r}\right) = 0, \tag{5}$$

that has to be fulfilled on Γ_x, with r being the radial direction. Together with the Eulerian equation of motion for compressible fluids,

$$\nabla \quad p = -\mathrm{i}\rho\omega\mathbf{v} \quad \text{or} \quad \frac{\partial p}{\partial \mathbf{n}} = -\mathrm{i}\rho\omega v_n, \tag{6}$$

and providing that the functions p fulfill the boundary condition (2) on S_D, the weak form of the boundary value problem reads

$$\int_{\Omega} \left(\nabla p \cdot \nabla q - k^2 pq\right) \, \mathrm{d}V + \int_{S_R} \mathrm{i}\rho\omega A_n pq \, \mathrm{d}S = -\int_{S_N} \mathrm{i}\rho\omega v_n^o q \, \mathrm{d}S, \quad (7)$$

with q being the weighting functions.

In order to find the Galerkin finite element formulation of the problem the discrete approximation of the pressure p on an element level of Ω for the interior and Ω_i for the exterior case is

$$p(\mathbf{x}, \omega) \approx \sum_{i=1}^{n} N_i(\mathbf{x}) p_i(\omega), \quad (8)$$

where N_i are known shape functions, $\mathbf{x}$ the coordinate vector, and p_i are unknown coefficients. The shape functions N_i give the local support with $N_i \in \mathbb{H}^1$ whereas $\cup N_i$ has to be globally C^0-continuous. For the exterior acoustic case the question of how to represent the semi-infinite domain Ω_e and to ensure the radiation condition (5) needs to be answered. Certainly, there are different options (see [30]) such as using the PML method [31, 32], the DtN-mapping [33, 34] to name just two. But for reasons that stem from the application the work has been motivated by, e.g. the interest in the solution in Ω_e, infinite elements are chosen [24, 25, 35, 36, 37, 38, 39, 40, 41] [2].

Paricularly the conjugated Astley-Leis formulation [42, 43, 44, 45, 46] is used here because it ensures uniqueness of the solution, due to the Petrov-Galerlin scheme the wave number dependent oscilatory terms are removed form the formulation with positive impact in the integration procedure and conditioning, they exhibit superior far field accuracy, and are most versatile with respect to the shape of the envelope Γ_x. An in depth explanation of these features is beyond the scope of this paper and the reader is referred to the provided references (see e.g. [5, 47]). Here, only the pressure approximation in Ω_e is stated in local coordinates s, t and v,

$$p \approx \sum_{i=1}^{n} \mathrm{p}_i \Phi_i(s,t,v) \, \exp^{-\mathrm{i}k\mu(s,t,v)}, \quad (9)$$

where v is the outward direction, n is the number of unknown degrees of freedom p_i that are assigned to the corresponding element. μ is a phase term and the shape functions Φ_i are given by

$$\Phi_i = \frac{(1-v)}{2} S_j(s,t) \; P_k(v), \quad (10)$$

[2] As opposed to the FEM/IFEM concept, the BEM approach could have been adopted especially since the recent improvements, namely Multipol-BEM, allow for the very efficient application of iterative solvers as well. However, this method is generally more restrictive since the entire acoustic fluid is assumed to be homogenous. This would prevent possible extensions of the considered application such as accounting for the flow field around the tire or inhomogeneous density distributions that stem from other noise mechanisms such as air-pumping.

Table I. Acoustic element matrices (K-acoustic stiffness matrix, M-acoustic mass matrix, C-acoustic damping matrix, f-acoustic load vector) for interior domain Ω_i and for exterior domain Ω_e.

	Ω_i	Ω_e
K	$\int_{\Omega^e} \nabla N_i \nabla N_j \, \mathrm{d}V$	$\int_{\Omega^e} (\nabla D\Phi_i + \nabla\Phi_i D)\, \nabla\Phi_j \, \mathrm{d}V$
M	$\int_{\Omega^e} N_i N_j \, \mathrm{d}V$	$\int_{\Omega^e} (1 - (\nabla\mu\nabla\mu))\, \Phi_i\Phi_j D \, \mathrm{d}V$
C	$\int_{S_R^e} A_n \rho c N_i^s N_j^s \, \mathrm{d}S$	$\int_{\Omega^e} (\nabla\mu\nabla\Phi_j) D\Phi_i - (\nabla D\nabla\mu)\Phi_i\Phi_j - (\nabla\Phi_i\nabla\mu) D\Phi_j \, \mathrm{d}V + \int_{S_R^e} A_n \rho c \Phi_i^s \Phi_j^s D \, \mathrm{d}S$
f	$\int_{S_N^e} v_n^o N_i^s \, \mathrm{d}S$	

where S_j is a shape function in the base of the element and P_k is a radial shape function.

As mentioned before, if a Galerkin procedure is employed for the finite element part of Ω and a Petrov-Galerkin procedure with the additional weighting factor $D = ((1-v)/2)^2$ for the potential infinite element part Ω_e, equation (7) yields a linear system of equations of the form

$$\mathbf{A}(k) \; \mathbf{p} := \left[\mathbf{K} + \mathrm{i}k\mathbf{C} - k^2\mathbf{M}\right] \; \mathbf{p} = -\mathrm{i}\rho ck \; \mathbf{f}, \quad (11)$$

where $\mathbf{K}$, $\mathbf{C}$, and $\mathbf{M}$ are acoustic stiffness, damping and mass matrix, respectively. The vector $\mathbf{p}$ contains the unknown coefficients for the pressure approximation p_i in (8) and $\mathbf{f}$ is the load vector. The contribution of an element e to the system matrices and the load vector is given in Table I.

3. Trial functions based on ultraspherical polynomials

3.1. Background

The resulting parameterized linear system of equation (11) is

- complex,
- indefinite,
- non-hermitian,
- non-normal,
- non-symmetric,
- and has an operator $\mathbf{A}$ which is quadratically dependent on the wave number k.

Due to the size of the applications that are to be considered, iterative methods will be used for the solution process. For simpler cases, such as symmetric and positive matrices, convergence theory is well established. For instance for GMRES the residual $\mathbf{r}_m = \mathbf{A}\mathbf{p}_m - \mathbf{b}$ at the iteration m and for the right hand side $\mathbf{b} = -\mathrm{i}\rho ck \; \mathbf{f}$ can be bounded by the condition number $cond(\mathbf{A})$ of $\mathbf{A}$ by

$$\|\mathbf{r}_m\| \le \left(\frac{cond(\mathbf{A})^2 - 1}{cond(\mathbf{A})^2}\right)^{m/2} \|\mathbf{r}_0\|. \quad (12)$$

For the type of matrices that evolve from the outlined modeling of the problem, the solution step is much more challenging. Usable convergence bounds ([48] and references therein) that are sharp enough are not yet available [49, 50]. The convergence still depends on eigenvalues [51] though, but not exclusively [52, 53, 54]. In [55] it has been observed, that beside the condition number the "degree of indefiniteness" of the system matrix is a strong influencing factor for the speed of convergence of the iterative solver. That is why the idea of the paper is to build on [55] and to define higher order elements based on polynomial bubbles that lead to an improved conditioning of the system matrix **A** by controlling the degree of indefiniteness, i.e. $min(\mathcal{R}\{\lambda(\mathbf{A})\})$. It has to be mentioned, that for the infinite elements the modifications of the formulation is restricted to the basis approximation $S_j(s,t)$ (see equation (10)) and for the approximation in radial direction $P_k(v)$ it is relied on the work of Dreyer et al. [56, 57].

In order to achieve the desired effect, only the basis for the higher order polynomial space is changed. This means the quality of the discretization is not changed when compared to standard *p*-FEM formulations, but the system matrix **A** itself is altered. Possibly, this not only changes the behaviour of the iterative solvers but also the quality of the final solution. The reason is because the solver minimizes the norm of the residual $\|\mathbf{r}_m\|$, which relates to the norm actual error of the solution $\|\mathbf{e}_m\|$ at the *m*-the iterate via

$$\begin{aligned} \mathbf{A}\mathbf{e}_m &= \mathbf{A}(\mathbf{p}-\mathbf{p}_m) \qquad (13)\\ &= \mathbf{b}-\mathbf{A}(\mathbf{p}_0+\mathbf{p}_m)\\ &= \mathbf{r}_0-\mathbf{A}\mathbf{p}_m)\\ &= \mathbf{r}_m\\ \|\mathbf{e}_m\| &= \|\mathbf{A}^{-1}\mathbf{r}_m\| \qquad (14)\\ &\le \|\mathbf{A}^{-1}\|\cdot\|\mathbf{r}_m\|, \end{aligned}$$

where $\mathbf{p}$ is the unknown exact solution and $\mathbf{p}_0$ the initial guess. For this reason the error needs to be checked later to ensure that the accuracy is not influenced negatively.

3.2. Basic Idea

As mentioned earlier, bubble functions will be used for the higher order terms in combination with standard linear nodal shape functions in order to ensure inter element continuity. The construction of the bubbles is based upon two ideas. First, the concept of the Heinrichs-basis is adopted (see [58] and references therein). This means the 1-D bubble shape function g_i of order i is defined by

$$g_i = (1-\xi^2)\, G^{(i-2)} \quad \text{for} \quad 2 \le i \le p, \qquad (15)$$

where $\xi \in [-1,1]$ is the natural coordinate[3].

Boyd [58] used Chebyshev polynomials for G and showd that this kind of bubble definition reduces the conditioning of the matrices containing the derivatives, because the common oscillations at the intervall boundaries are reduced. Besides exploiting this effect, the choice of G will be different. Here, for the formulation of G the idea of the standard *p*-FEM formulation based on integrated Legendre polynomials [19] is followed, where the polynomial basis is chosen such that the definition of the stiffness matrix matches the orthogonality condition. In the case of the Helmholtz equation this gives superior performance at low frequencies (see [55]) because the contribution of the stiffness matrix **K** in **A** (11) dominates. Since for this paper the computations at elevated frequencies are of interest, it is focussed on the mass matrix **M** because this contribution exhibits quadratic frequency dependence. This means it is aimed for finding polynomial basis functions G such that the bubble part of the mass matrix,

$$m_{ij} = \int_{-1}^{1} (1-\xi^2)^2 G_i G_j \,\mathrm{d}\xi \quad \text{for} \quad i,j \ge 2, \qquad (16)$$

matches the orthogonality condition of this basis. If generally orthogonality of two functions $x(\xi)$ and $y(\xi)$ is defined by

$$\langle x_n, y_m \rangle = \delta_{mn} {v_n}^2, \qquad (17)$$

with the Kronecker δ-function, the normalization constants v_n and the inner product

$$\langle x_n, y_m \rangle = \int_{-a}^{b} w(\xi)x(\xi)y(\xi)\,\mathrm{d}\xi. \qquad (18)$$

Then the task is to find polynomial basis functions $G(\xi)$ that are orthogonal with respect to the weight $w(\xi) = (1-\xi^2)^2$. This can be found within the class of Gegenbauer or ultrasperical polynomials ${P_n}^{(\lambda)}$, which is a descendant of the Jacobi polynomials ${P_n}^{(\alpha,\beta)}$ with $\alpha = \beta = \lambda - \frac{1}{2}$ [59]. The weight for which the ultraspherical polynomials ${P_n}^{(\lambda)}(\xi)$ are orthogonal is $w^{(\lambda)}(\xi) = (1-\xi^2)^{\lambda-\frac{1}{2}}$. This means if the Gegenbauer polynomials with $\lambda = \frac{5}{2}$ are chosen for G, the desired property is met.

As an intermediate check, the influence of the new element formulation on the considered matrix properties is determined for a a 1-D master element. It is compared with the standard formulation based on integrated Legendre polynomials and with the element formulation based on Bernstein polynomials since the latter one has been shown to be very efficient in the past [55, 60, 61]. The effect of the improved basis functions on the condition of the mass and stiffness matrix is given in Figure 3.

As mentioned before, the standard hierarchical basis has been desiged with the focus on the stiffness matrix, so it gives the best condition number. But the desired effect of the new formulation is apparent with showing much better conditioning than the Bernstein elements for the stiffness matrix. As for the mass matrix, the Gegenbauer elements result in the best condition number for orders larger than

[3] For the sake of simplicity only the 1-D formulation is presented here and ξ is used as a generalized natural coordinate that can be replaced by any entity of the coordinate vector $\mathbf{x}$ according to equation (8). Following the standard hierarchical *p*-FEM formulation of Szabo and Babuška [19] the multidimensional shape functions then just result from the tensor product of the one dimensional counterparts. This gives the well-known edge-bubbles and interior bubbles next to the nodal functions whereas global C^0-continuity is preserved.

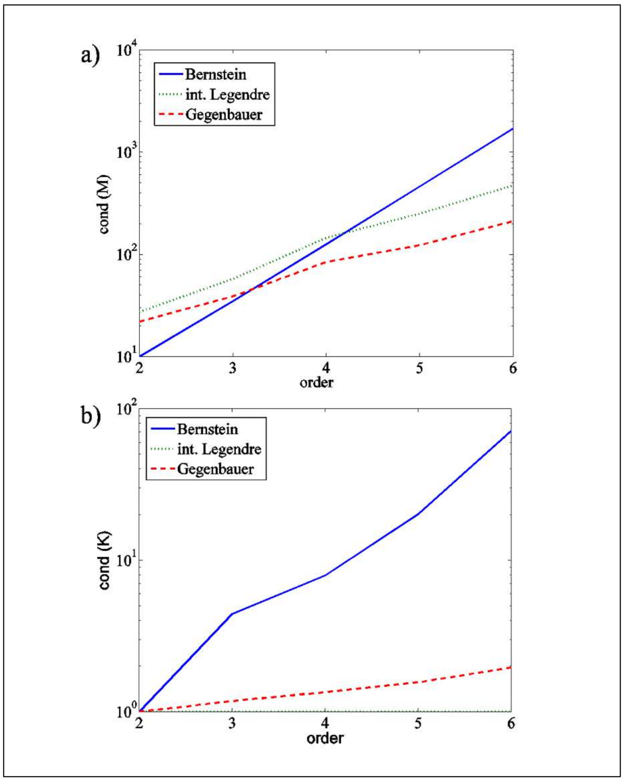

Figure 3. Comparison of the condition number of the mass matrix (a) and the stiffness matrix (b) for different element formulations.

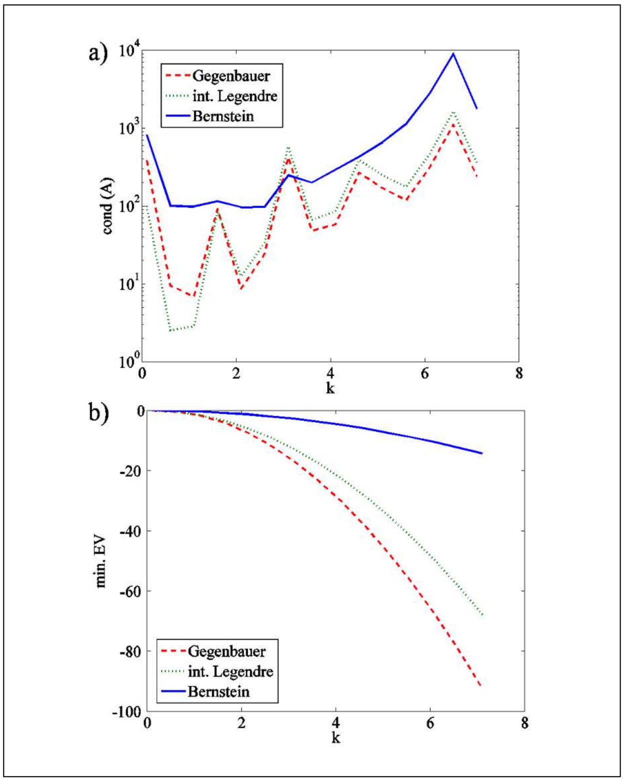

Figure 4. Condition number (a) and min. eigen value λ_{min} (b) of the system matrix A resulting from a 1-D master element of order six.

three. The accumulative effect on the system matrix **A** can be seen in Figure 4.

As expected, the elements based on integrated Legendre polynomials have the best conditioning of **A** for small wave numbers, but with increasing wave number the Gegenbauer elements outperform the other formulation[4]. If the degree of indefiniteness is considered. it has to be noticed that the new formulation is inferior. This gave rise to the following section, where the element basis functions have been slightly changed as a remedy of this issue.

Before though, the question of accuracy, as raised by equation (14), will be adressed. For the so far considered small 1-D problem the term $\|\mathbf{A}^{-1}\|$ can in fact be computed and the results for the 2-norm are exemplarily depicted for the wave number $k = 6$ in Figure 5.

(The results for the standard elements are omitted because they are identical to the Gegenbauer elements.) It can be seen that $\|\mathbf{A}^{-1}\|$ is smaller for all approximation orders. According to equation (14), this yields the conclusion, that the error of the solution after the iterative process converged is for the Gegenbauer elements at least as good as for the Bernstein elements.

[4] The general oscillatory behavior of cond(A) in Figure 4a) originates in the fact, that the discrete frequencies chosen for the evaluation, are more or less close to the value, where one eigen-value of the matrix A becomes 0 and hence, the condition number becomes infinite (Since the spectrum of A shifts towards the negative half-plane with increasing wave number, the eigen-values switch signs and thus, pass 0).

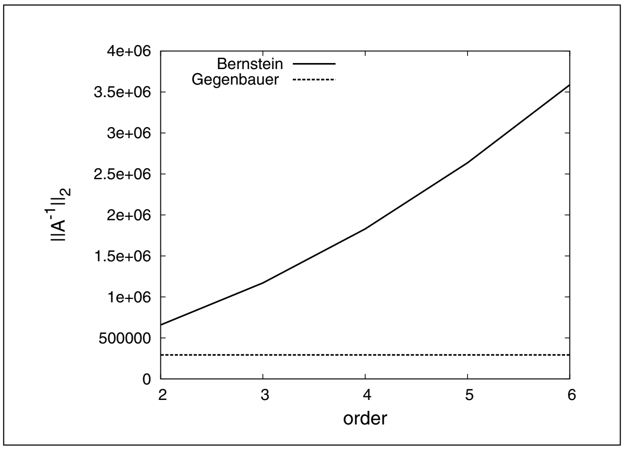

Figure 5. 2-norm of the inverse of the system matrix A (resulting from a 1-D master element at $k = 3$) for different FE-formulations and approximation orders.

3.3. Adaption of the formulation

As mentioned before, the proposed element formulation does not exhibit the desired properties with respect to $\min(\mathcal{R}\{\lambda(\mathbf{A})\})$ of the corresponding system matrix **A**. As the source of the problem the second order term $g_2(\xi)$ has been identified. Since the Bernstein elements showd good properties up to order two (see also Figure 3a)), it has been decided to modify the formulation slightly by changing the terms $g_i, i = 0, 1, 2$ to the Bernstein basis. This gives the modified Gegenbauer formulation $\tilde{g}_i(\xi)$ that can be un-

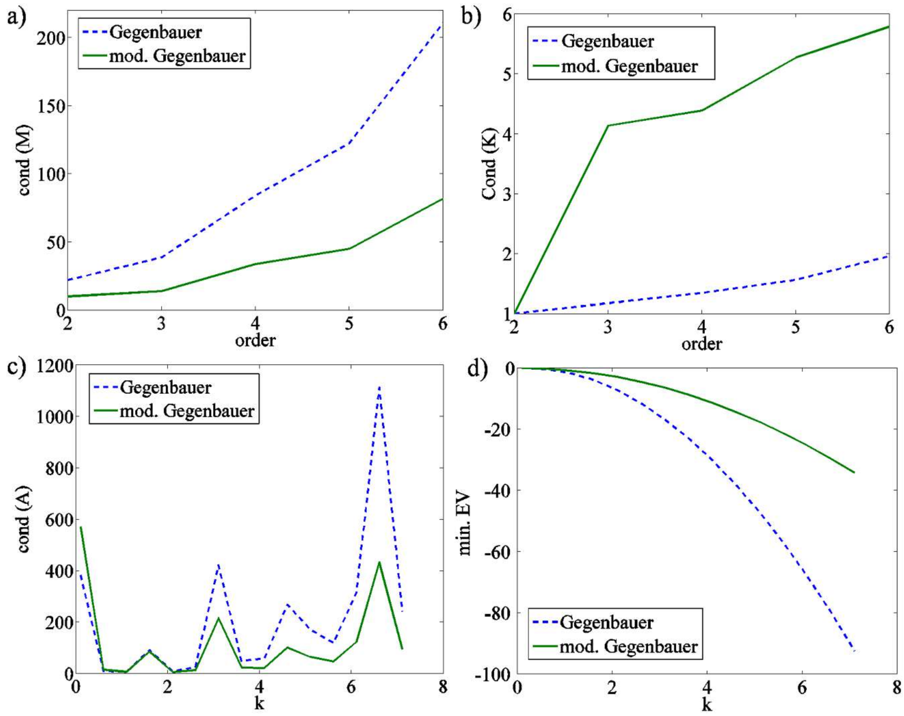

Figure 6. Effect of the modification of the Gegenbauer elements; Change of the condition number of M (a), change of the condition number of K (b), change of cond(A) for a sixth order 1-D master element (c), change of min. eigenvalue of A for a sixth order 1-D master element (d).

derstood as a second order Bernstein element enriched by higher order bubbles based on normalized ultraspherical polynomials $G(\xi)$ as proposed before. The basis functions now read

$$\begin{aligned} \tilde{g_0} &= \frac{1}{4}(1-\xi)(1-\xi), \\ \tilde{g_1} &= \frac{1}{4}(1+\xi)(1+\xi), \\ \tilde{g_2} &= \frac{1}{2}(1-\xi)(1+\xi), \\ \tilde{g_i} &= (1-\xi^2)G^{(i-2)} \quad \text{for} \quad 3 \le i \le p. \end{aligned} \tag{19}$$

That this modification changed the desired spectral element properties can be seen in Figure 6.

Finally, two scaling factors, c_f for the second order term and c_k for the higher order bubbles are introduced:

$$\begin{aligned} \tilde{g_2} &= c_f \, \frac{1}{2}(1-\xi)(1+\xi) \\ \tilde{g_i} &= c_k \, (1-\xi^2)G^{(i-2)} \quad \text{for} \quad 3 \le i \le p. \end{aligned} \tag{20}$$

It has to be emphasized that these factors do not arise from the core idea of this paper, so they could both be chosen to one, but they provide an additional measure to tune the fomulation. The effect can be revealed when looking at the derivative of the bubbles that stiffness matrix consists of,

$$\tilde{g_i}' = -2 \, c_k \, \xi \, G^{(i-2)} + c_k \, (1-\xi^2) \, G\prime^{(i-2)} \quad \text{for} \quad 3 \le i \le p. \tag{21}$$

Depending on the choice of c_k, the realtive contribution of the function value $G^{(i-2)}$ and its derivative $G'^{(i-2)}$ can be changed. Again, the 1-D master element is utilized to demonstrate the general effect of the variation of these parameters. Exemplary, Figure 7 shows the results for a sixth order element and wave number $k = 3$ (In fact the characteristics of the curves have been the same for different wave numbers and orders of approximation). The actual selection of the parameter combination will be based on the effect on the convergence of the iterative solution strategy for a specific acoustical problem and will be part of the next section.

4. Numerical Examples

So far, the new element formulation has been derived on the basis of some spectral properties of the discretized system that are only indicators for the convergence of iterative solvers. Now, some testing is required to see if the desired effect of speeding up convergence of the solver actually occurs. Therefor, a rather small academic test problem is used first, since it allows for an accessment with passable computational effort and in turn, to tune the parameters c_f and c_k introduced in the previous section. Finally, the effect of the formulation will be demonstrated by two large scale industrial acouistcal applications, an interior and an exterior one.

All computations have been conducted using the finite element library libMesh [62]. For the solver BICGSTAB

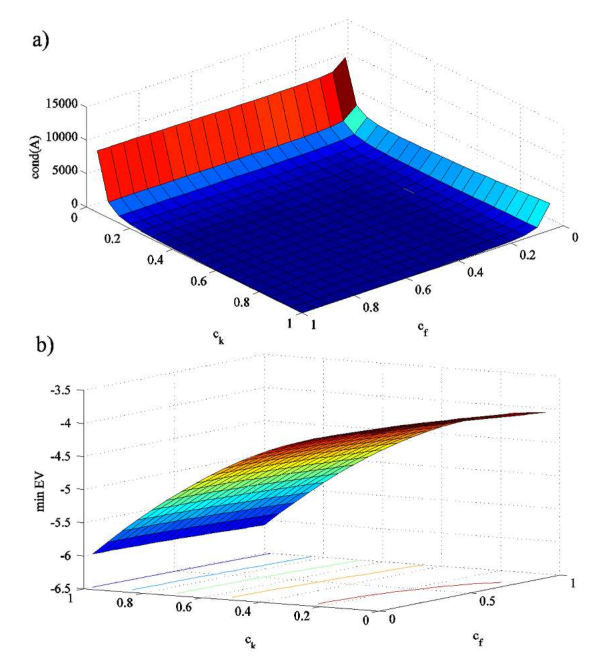

Figure 7. The effect of variations of the parameters c_f and c_k on the condition number (a) and the smallest eigen value (b) of a system matrix resulting from a 1-D master element of order six for wave number $k = 3$.

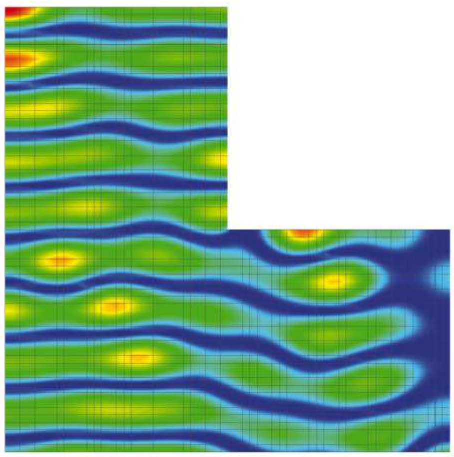

Figure 8. L-shaped acoustical cavity with a QUAD-mesh used for 4th order FE-approximation and a contour plot of the pressure amplitude at 1500 Hz.

[63] and as a preconditioner ASM [64] have been used because this combination has previously been found to work best for this type of application. The actual implementation has been taken from the library PetSc [65]. As convergence criterion a reduction of the relative residual $\|\mathbf{r}_m\|/\|\mathbf{b}\|$ by 10^{-6} has been used throughout this section.

4.1. Preliminary numerical asseessment

As the initial acadamic example a L-shaped acoustic domain with an edge length of 1m as depicted in Figure 8 has been used. The mesh has been adapted such that for each investigated order of approximation (2 to 6) the number of degrees of freedom (dof) has a constant value of $11,041$. The botton has been excited within a frequency range of 50 Hz to 1500 Hz in steps of 50 Hz. First, the sellection of the parameters c_f and c_k has been based on comparing the accumulative iteration counts for the considered frequency sweep for each combination of $c_f,\ c_k \in [0.05, 1]$ with steps of 0.05. Figure 9a) shows exemplarily the result for the sixth order approximation and, for the sake of presentability, only a selected set of parameter combinations. As a result of these computations $c_f = 0.8$, $c_k = 0.1$ has been the final choice. By selecting the parameters based on this specific problem, no generality is claimed. But first, it is not required that these factors have to be used at all. This investigation is only meant to give an impression on their influence on the solver performance. Second, the chosen combination prooved to work well for other problems as well, such as the ones presented in the next subsection.

In Figure 9b the savings in computational cost when using the new elements compared to the Bernstein elements as a benchmark are shown. It can be seen, that with increasing order the overall gain in computational efficiency becomes larger. This is due to the orthogonality property that the element basis has been derived from, and the fact, that the number of bubble functions grow quadratically with the polynomial degree and thus, form the major part of the basis with increasing order.

Opposed to the so far presented accumulative comparisons, Figure 10 shows the frequency dependent comparison of the different element formulations. Additionally, Figure 11 shows the accumulated L_2-error for different orders of approximation, i.e. the L_2-error added for all computed frequencies. It has to be noted that the solution of a simulation with fifth order approximation on a finer grid, resulting in $97,921$ dof, has been used as the reference solution, since an analytical solution is not available for this problem.

On the one hand it can be seen, as expected, that an increase of approximation order, while keeping the number of dofs constant, gives a more accurate solution. On the other hand it can be concluded that both element formulations yield a solution with the same accuracy, so that the reasoning derived from Figure 5 and equation (14) is valid and the increase in computational efficiency happens not at the expense of accuracy.

It has to be mentioned that from here on, the final formulation of modified Gegenbauer elements is referred to Gegenbauer elements for the sake of brevity.

4.2. Practical numerical examples

Finally, the impact of the presented element formulation should be demonstrated on two 3-D large scale industrial applications. As an interior accoustic representant the car compartment depicted in Figure 12 has been used. The model consists of 41097 hexahedral elements with 27 nodes each, leading to 351569 nodes in total. Simulations

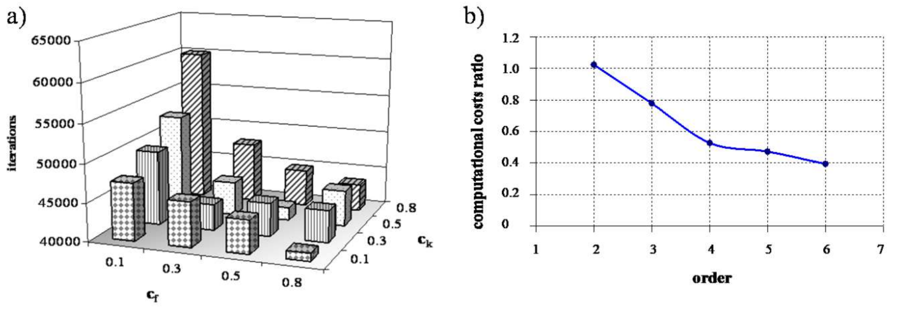

Figure 9. (a) Total number of iterations required for a acoustical simulation of a L-shaped domain between 50 Hz and 1500 Hz for different parameter combinations of c_f and c_k and a sixth order of approximation (b); The ratio of the total number of iterations required for an acoustical simulation of a L-shaped domain between 50 Hz and 1500 Hz of the new element formulation and the Bernstein elements as a benchmark for orders of approximation between two and six.

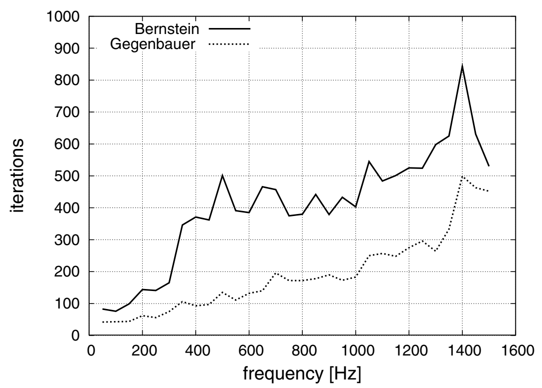

Figure 10. Comparison of the iterations required for the solution of the L-shaped problem using Bernstein and Gegenbauer elements for fourth order approximation.

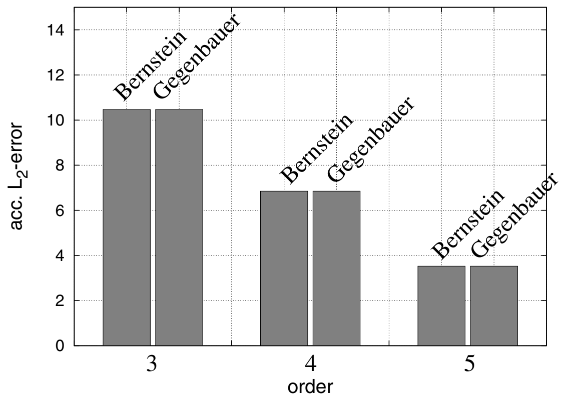

Figure 11. Comparison of the L_2-error accumulated for the entire considered frequency sweep for different orders of approximation.

have been conducted for 3rd and 4th order elements leading to 1.16 Mio. and 2.72 Mio. degrees of freedom.

Table III shows the savings in computational costs in percent of the reference solution with Bernstein elements.

The last example of exterior acoustic nature is the simulation of tire rolling noise. Figure 13 shows the convex envelope mesh of a tire where the infinite elements are "attached" to.

In total the mesh contains 20 240 elements. Using a third order FE/IFE-basis approximation and sixth order IFE-radial approximation leads to 910 820 degrees of freedom. The solution of the problem comprises several hundred single steps, namely for every frequency contained in the excitation spectrum of the road within the considered range. Here, a frequency range between 1000 Hz and 1500 Hz has been investigated which caused 137 subsequent systems of equations to be solved. Figure 14 compares the frequency dependent iterations required for each solution step. In this case the new formulation yields only 65% of the computational costs when the total numbers of iterations for the entire frequency range are compared.

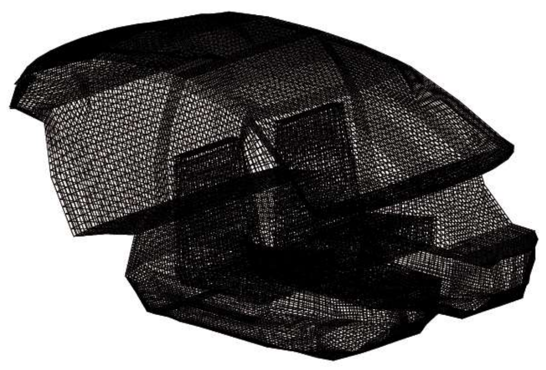

Figure 12. Discretization of a car compartment with 41097 HEX27 elements.

It can be noticed, that for both examples the new formulation was more efficient and that the savings in computational costs have even been slightly better than the values determined for the 2-D case (see Figure 9).

Table II. Comparison of the iterations required to obtain a solution for a car compartment at different frequencies, 3rd or 4th orders of approximation and element formulations.

	500 Hz		750 Hz	
Element type	3rd	4th	3rd	4th
Gegenbauer	3 037	3 855	5 251	6 364
Bernstein	4 989	8 263	7 380	11 036

Table III. Computational savings for the simulation of a car compartment when using Gegenbauer elements compared to Bernstein elements

Frequency	iterations [%]	
[Hz]	3rd order	4th order
500 Hz	39.1	53.3
750 Hz	28.8	42.3

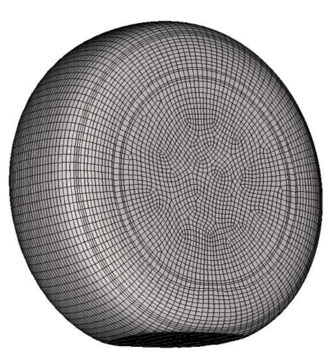

Figure 13. Tire envelope mesh with 10.120 HEX27 elements.

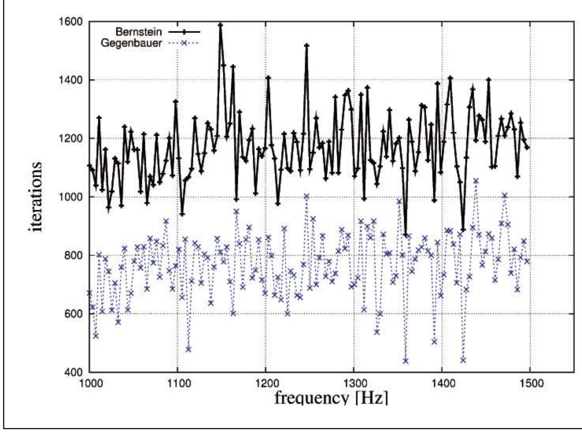

Figure 14. Comparison of the iterations required for the solution of tire rolling noise between 1000 Hz and 1500 Hz when using Bernstein or Gegenbauer elements.

The actual saving in computational time certainly depends on the hardware used. Here, computations have been conducted on a small Linux cluster with 24 AMD Opteron 250 processors, which lead to savings in the order of magnitude of one and a half days for the tire noise simulation run and of about three days for the fourth order car compartment case.

5. Conclusions

The current work aimed to obtain a *p*-FEM formulation that improves the convergence of Krylov subspace iterative methods, which are used for the solution of the discretized weak form of the Helmholtz equation. As opposed to other element formulation improvements which mostly try to reduce the dispersion error, there is no unique criterion a new formulation can target at in order to achieve the described behaviour. Here, it has been chosen to improve conditioning and the degreee of indefiniteness of the resulting system of equation. As a result of these considerations ultraspherical polynomials have been introduced for the formulation of acoustical finite and infinite elements, hence, using the same polynomial solution space as standard methods but changing the basis of this space. Numerical tests showed that this measure indeed gives an improved numerical efficiency by at least the same accuracy. When elements based on Bernstein polynomials, a formulation that has been previously proven to be computationally by far more efficient than standard methods based on integrated Legendre polynomials, are used as a benchmark, the new elements allow for an additional improvement of the numerical performance by a factor between 1.25 and 2.15 for element orders between three and six. particularly, this has been confirmed by large-scale 3-D models of practical relevance.

References

[1] O. Zienkiewicz: Achievements and some unsolved problems of finite element method. International Journal for Numerical Methods in Engineering **47** (2000) 9–28.

[2] I. Babuška, F. Ihlenburg, E. T. Paik, S. A. Sauter: A generalized finite element method for solving the helmholtz equation in two dimensions with minimal pollution. Computer Methods in Applied Mechanics and Engineering **128** (1995) 325 – 359.

[3] I. Babuška, S. A. Sauter: Is the pollution effect of the FEM avoidable for the Helmholtz equation considering high wave numbers? SIAM Journal on Numerical Analysis **34** (1997) 2392–2423.

[4] K. Gerdes, F. Ihlenburg: On the pollution effect in fe solutions of the 3d-helmholtz equation. CMAME **170** (1999) 155–172.

[5] I. Harari: A survey of finite element methods for time-harmonic acoustics. Computer Methods in Applied Mechanics and Engineering **195** (2006) 1594–1607.

[6] R. Azis, A.and Kellogg, A. Stephens: A two point boundary value problem with a rapidly oscillating solution. Numer. Math. **53** (1988) 107–121.

[7] E. Perrey-Debain, O. Laghrouche, P. Bettess, J. Trevelyan: Plane-wave basis finite elements and boundary elements for three-dimensional wave scattering. Philosophical Transactions: Mathematical, Physical and Engineering Sciences **362** (2004) 561–577.

[8] O. Laghrouche, P. Bettess, R. J. Astley: Modelling of short wave diffraction problems using approximating systems of plane waves. International journal for numerical methods in engineering. **54** (August 2002) 1501–1533.

[9] T. Strouboulis, I. Babuška, K. Copps: The design and analysis of the generalized finite element method. Computer Methods in Applied Mechanics and Engineering **181** (2000) 43–69.

[10] I. Babuška, U. Banerjee, J. Osborn: Generalized finite element methods: Main ideas, results, and perspective. Tech. Rept. 0408, Institute for Computational Engineering and Sciences, University of Texas, Austin, Texas, 2004.

[11] L. Franca, C. Farhat, A. P. Macedo, M. Lesoinne: Residual-free bubbles for the helmholtz equation. International Journal for Numerical Methods in Engineering **40** (1997) 4003–4009.

[12] P. Barbone, I. Harari: Nearly h1-optimal finite element methods. Computer Methods in Applied Mechanics and Engineering **190** (2001) 5679–5690.

[13] C. Farhat, I. Harari, L. P. Franca: The discontinuous enrichment method. Computer Methods in Applied Mechanics and Engineering **190** (2001) 6455–6479.

[14] C. Farhat, I. Harari, U. Hetmaniuk: The discontinuous enrichment method for multiscale analysis. Computer Methods in Applied Mechanics and Engineering **192** (2003) 3195 – 3209.

[15] R. Tezaur, C. Farhat: Three-dimensional discontinuous Galerkin elements with Lagrange multipliers for the solution of mid-frequency Helmholtz problems. International Journal for Numerical Methods in Engineering **66** (2006) 796–815.

[16] R. Hiptmair, A. Moiola, I. Perugia: Plane wave discontinuous galerkin methods for the 2d helmholtz equation: Analysis of the p-version. SIAM J. Numerical Analysis **49** (2011) 264–284.

[17] O. Cessenat, B. Despres: Application of an ultra weak variational formulation of elliptic pdes to the two-dimensional helmholtz problem. SIAM Journal on Numerical Analysis **35** (1998) 255–299.

[18] T. Huttunen, P. Monk, J. P. Kaipio: Computational aspects of the ultra weak variational formulation. Journal of Computational Physics **182** (2002) 27–46.

[19] B. A. Szabo, I. Babuška: Finite element analysis. Wiley, Chichester, 1991.

[20] B. Szabo, A. Duester, E. Rank: Encyclopedia of computational mechanics. volume 1: Fundamentals. John Wiley and Sons, Ltd, 2004.

[21] S. Adjerid, M. Aiffa, J. E. Flaherty: Hierarchical finite element bases for triangular and tetrahedral elements. Computer Methods in Applied Mechanics and Engineering **190** (2001) 2925–2941.

[22] T. Hughes, G. Feijó, L. Mazzei, J.-B. Quincy: The variational multiscale methodâĂŤa paradigm for computational mechanics. Computer Methods in Applied Mechanics and Engineering **166** (1998) 3 – 24. <ce:title>Advances in Stabilized Methods in Computational Mechanics</ce:title>.

[23] T. Hughes: Multiscale phenomena: Green's functions, the dirichlet-to-neumann formulation, subgrid scale models, bubbles and the origins of stabilized methods. Computer Methods in Applied Mechanics and Engineering **127** (1995) 387 – 401.

[24] F. Ihlenburg: On fundamental aspects of exterior approximations with infinite elements. Journal of Computational Acoustics **8** (2000) 63–80.

[25] L. Demkowicz, K. Gerdes: Convergence of the infinite element methods for the helmholtz equation in separable domains. Numerische Mathematik **79** (1998) 11–42.

[26] F. Ihlenburg, I. Babuška: Finite element solution of the Helmholtz equation with high wave number part II: The *h-p* verson of the FEM. SIAM Journal on Numerical Analysis **34** (1997) 315–358.

[27] F. Ihlenburg: The medium-frequency range in computational acoustics: Practical and numerical aspects. Journal of Computational Acoustics **11** (2003) 175–193.

[28] J. Biermann, O. von Estorff, S. Petersen, H. Schmidt: Computational model to investigate the sound radiation from rolling tires. Tire Science and Technology **35** (2007) 209–225.

[29] J. Biermann, E. de Sturler: Acceleration of acoustical computations by using iterative solvers with krylov subspace recycling. International Journal for Numerical Methods in Engineering **submitted** (2011).

[30] D. Givoli: High-order local non-reflecting boundary conditions: a review. Wave Motion **39** (2004) 319–326.

[31] J.-P. Bérenger: A perfectly matched layer for the absorption of electromagnetic waves. Journal of Computational Physics **114** (1994) 185–200.

[32] E. Turkel, A. Yefet: Absorbing pml boundary layers for wave-like equations. Applied Numerical Mathematics **27** (1998) 533–557.

[33] J. B. Keller, D. Givoli: Exact non-reflecting boundary conditions. Journal of Computational Physics **82** (1989) 172–192.

[34] M. J. Grote, J. B. Keller: On nonreflecting boundary conditions. Journal of Computational Physics **122** (1995) 231–243.

[35] P. Bettess: Infinite elements. Penshaw Press, 1992.

[36] D. S. Burnett, R. L. Holford: Prolate and oblate spheroidal acoustic infinite elements. Computer Methods in Applied Mechanics and Engineering **158** (1998) 117–141.

[37] D. S. Burnett, R. L. Holford: An ellipsoidal acoustic infinite element. Computer Methods in Applied Mechanics and Engineering **164** (1998) 49–76.

[38] J. J. Shirron, I. Babuška: A comparison of approximate boundary conditions and infinite element methods for exterior Helmholtz problems. Computer Methods in Applied Mechanics and Engineering **164** (1998) 121–139.

[39] K. Gerdes: The conjugate vs. the unconjugate infinite element method for the helmholtz equation in exterior domains. Computer Methods in Applied Mechanics and Engineering **152** (1998) 125–145.

[40] J. J. Shirron, S. Dey: Acoustic infinite elements for non-separable geometries. Computer Methods in Applied Mechanics and Engineering **191** (2002) 4123–4139.

[41] K. Gerdes: A review of infinite element methods for exterior Helmholtz problems. Journal of Computational Acoustics **8** (2000) 43–62.

[42] R. J. Astley, G. J. Macaulay, J.-P. Coyette, L. Cremers: Three-dimensional wave-envelope elements of variable order for acoustic radiation and scattering. Part I.Formulation in the frequency domain. Journal of the Acoustical Society of America **103** (1998) 49–63.

[43] R. J. Astley: Infinite element formulations for wave problems: a review of current formulations and an assessment of accuracy. International Journal for Numerical Methods in Engineering **49** (2000) 951–976.

[44] R. J. Astley, J. A. Hamilton: Numerical studies of conjugated infinite elements for acoustic radiation. Journal of Computational Acoustics **8** (2000) 1–24.

[45] R. J. Astley, J.-P. Coyette: The performance of spheroidal infinite elements. International Journal for Numerical Methods in Engineering **52** (2001) 951–976.

[46] R. J. Astley, J.-P. Coyette: Conditioning of infinite element schemes for wave problems. CNME **17** (2001) 31–41.

[47] L. L. Thompson: A review of finite-element methods for time-harmonic acoustics. Journal of the Acoustical Society of America **119** (2006) 1315–1330.

[48] I. Ipsen: Expressions and bounds for the gmres residual. BIT **40** (1999) 524–533.

[49] N. Gmati, B. Philippe: Comments on the gmres convergence for preconditioned systems. – In: Large-Scale Scientific Computing. I. Lirkov, S. Margenov, J. Waśniewski (eds.). Springer-Verlag, Berlin, Heidelberg, 2008, 40–51.

[50] M. Embree: How descriptive are gmres convergence bounds? Tech. Rept. Oxford University Computing Laboratory, 1999.

[51] S. Eisenstat, H. Elman, M. Schultz: Variational Iterative Methods for Nonsymmetric Systems of Linear Equations. SIAM J. Num. Anal. **20** (1983) 345–357.

[52] A. Greenbaum, Z. Strakos: Matrices that generate the same krylov residual spaces. in Recent Advances in Iterative Methods, 1994, Springer, 95–118.

[53] A. Greenbaum, Z. Strakos: Any nonincreasing convergence curve is possible for gmres. SIAM J. Matrix Anal. Appl **17** (1996) 465–469.

[54] N. M. Nachtigal, S. C. Reddy, L. N. Trefethen: How fast are nonsymmetric matrix iterations. SIAM J. Matrix Anal. Appl. **13** (July 1992) 778–795.

[55] J. Biermann, O. von Estorff, S. Petersen, C. Wenterodt: Higher order finite and infinite elements for the solution of helmholtz problems. Computer Methods in Applied Mechanics and Engineering **198** (2009) 1171–1188.

[56] D. Dreyer, O. von Estorff: Improved conditioning of infinite elements for exterior acoustics. International Journal for Numerical Methods in Engineering **58** (2003) 933–953.

[57] D. Dreyer, P. S., O. von Estorff: Effectiveness and robustness of improved infinite elements for exterior acoustics. Computer Methods in Applied Mechanics and Engineering **195** (2006) 3591–3607.

[58] J. Boyd: Chebyshev and fourier spectral methods. Dover Pubn Inc., 2003.

[59] G. Szego: Orthogonal polynomials. 4th ed. ed. Providence, RI: Amer. Math. Soc., 1975.

[60] S. Petersen, D. Dreyer, O. von Estorff: Assessment of finite and spectral element shape functions for efficient iterative simulations of interior acoustics. Computer Methods in Applied Mechanics and Engineering **195** (2006) 6463–6478.

[61] S. Petersen: Adaptive finite and infinite Elementemethoden in der Akustik. Tech. Rept. PhD. Thesis, Hamburg University of Technology, 2006.

[62] B. S. Kirk, J. W. Peterson: `libMesh`. 2005. (last viewed 1/01/10).

[63] H. A. Van der Vorst: Bi-CGSTAB: A Fast and Smoothly Converging Variant of Bi-CG for the Solution of Nonsymmetric Linear Systems. SIAM Journal on Scientific and Statistical Computing **13** (1992) 631–644.

[64] M. Dryja, O. Widlund: An additive variant of the Schwarz alternating method for the case of many subregions. Tech. Rept. Computer Science Technical Report 339, Courant Institute, New York University, 1987.

[65] S. Balay, K. Buschelman, W. D. Gropp, D. Kaushik, M. Knepley, L. C. McInnes, B. F. Smith, H. Zhang: PETSc Web page. 2004. (last viewed 1/01/10).